

N79-19021

Paper No. 12

**EFFECTS OF HYPODYNAMIC SIMULATIONS ON
THE SKELETAL SYSTEM OF MONKEYS**

D. R. Young and J. W. Tremor, *Ames Research Center, NASA,
Moffett Field, California*

ABSTRACT

A research and development program has been undertaken to evaluate the skeletal losses of subhuman primates in hypodynamic environments. The goals of the program are: 1) to uncover the mechanisms by which weightlessness affects the skeletal system, 2) to determine the consequences and reversibility of bone mineral losses, and 3) to acquire a body of data needed to formulate an appropriate countermeasure program for the prevention of skeletal deconditioning. Space flight experiment simulation facilities are under development and will be tested for their capability in supporting certain of the requirements for these investigations.

INTRODUCTION

Losses of bone mineral have been observed in crew members during weightless space flight. Variations in calcium homeostasis were clearest during the 84-day Skylab mission, SL-4 (1). As shown in Figure 1, the urinary calcium excretion was elevated systematically, and there was a maximal loss of 7.9% of mineral content in the os calcis. In contrast, the radius and ulna did not change measurably.

The findings indicate that there is a loss of bone mineral during space flight despite the intake of relatively high levels of dietary calcium and phosphate, and despite physical exercise regimes which are extremely vigorous. Typically, weight-bearing bones appear to be significantly affected, whereas other portions of the skeletal system seem stable. Although the losses have not been of clinical concern, the basis for the alterations has not been explained adequately, and the consequences for passengers and crew members in future long-duration space flight have not been assessed.

Our studies have been directed towards the demonstration of a useful animal model for experimental testing and towards the verification of the underlying mechanisms of action in bone mass loss. Three factors have led us to select the experimental monkey for an animal model. First, there is available a reasonably good caliber of scientific information regarding subhuman primates, e.g., 1) the life support requirements for monkeys have been

defined and systems partially developed, 2) nutrition requirements in support of particular experiments have been delineated, 3) the biochemistry and physiology of the animal is similar to and approaches identity with man, thus facilitating the extrapolation of data between species. Second, flight experience has already been gained through suborbital space flights with squirrel monkeys and chimpanzees, and orbital flights with the chimpanzee and the pigtailed monkey (*M. nemestrina*). Third, reasonable animal supply sources, and pertinent information on primatology and disease control can be expected through the various national primate research institutes.

The selection of the monkey as an animal model for the calcium research program is further justified by reports which demonstrate a significant bone mass loss in the monkey caused by disuse osteoporosis, and other reports showing general similarities in the calcium metabolism of man and monkeys. For example, total body immobilization of the rhesus monkey (*M. mulatta*) for 2 months increases bone resorption in the long bones with a resultant loss of cortical bone (2). Immobilization decreased spinal impact tolerance by 33%; the mechanism of the resulting spinal injuries was related to a high incidence of intervertebral disk prolapse in the thoracic and lumbar vertebrae (3). The dynamics of the short-term blood calcium regulation are similar in man and the monkeys, (*M. mulatta* and *M. nemestrina*)(4). Calcitonin, a plasma calcium regulatory hormone, also lowers the blood calcium level in adolescent monkeys (*M. mulatta* and *M. fascicularis*) (5,6). The average bone formation rate in adolescent rhesus monkeys is 243 mg Ca/day (7), which is substantially similar to that observed in children and is at the lower range of values reported for normal adults (8).

PRIMATE RESTRAINT STUDIES

Procedures and Physiologic Responses

Our experimental approach has been to simulate hypodynamic and hypogravic environments for weight-bearing bones by restraining adult male monkeys (*M. nemestrina*) in a semirecumbent position according to the technique of Howard et al. (9) for varying periods of time. Figure 2 shows a restraint unit in a typical study of several weeks duration. Figure 3 shows the food (Purina) and water intake during 10 weeks of restraint. During the control phase of testing, the average food intake of seven monkeys was 147 ± 6 g/day/animal, which represents about 530 kcal. During the first 2-3 weeks of restraint, food intake was depressed but then returned to typical normal levels. Mean water consumption during the control period was 787 ± 244 ml/day and declined during restraint. Body weight was reasonably constant during the control phase of testing; variations of 6-12% in body weight were measured during restraint. Changes in the metabolism of body nitrogen and minerals are shown in Table 1, where comparisons of the average daily urinary output are made between restrained animals and body-weight-matched control animals given identical amounts of food and

water over a 10-week period. Urinary excretion in the restrained animals tended to be higher than that of the controls, especially during the last 5-6 weeks of restraint, and the restrained animals were also more variable. Urinary nitrogen and potassium were significantly higher (22%) in restrained animals; phosphorus excretion was increased by a factor of 3.8. Losses of nitrogen and electrolytes were also reported during the Apollo Missions, SL-3, and SL-4 and are associated with body mass loss.

Circulatory changes have also been observed. Therefore, blood volume changes were evaluated during one month of restraint. Blood volume was determined with ^{125}I -labeled albumin (RIHSA) measured in a Volemetron; the hematocrit was also measured. The responses were compared to a well-matched group of control monkeys. Figure 4 shows that the total blood volume decreased 11.7%. The red cell mass by itself decreased 12.0%, which is comparable to the 12% decrease found in SL-3 and the 10% decrease found in Apollo 14 and 17 crew members.

Bone Studies

Further comparison studies were undertaken to evaluate bone mineral losses in the monkey. The bone mineral content at a specific cross section was determined by the photon absorption technique (10) similar to that used to study astronauts. Ten animals were studied during 1 month of restraint. As compared to control animals, the restrained animals lost bone mineral content in the midshaft of the tibia. The mineral content of the distal radius and ulna was unchanged. Table 2 shows the losses in the tibia of the restrained animals. The average 3.5% loss was significant beyond the 5% level of confidence. The data correlate with the results obtained in the Skylab flights. For example, bone mineral decreased 5-7% in the os calcis of one SL-3 (59-1/2-day flight) crewman and two of the SL-4 (84-day flight) crew members.

The bone mineral loss in the experimental monkeys tends to be regional. Figure 5 shows the typical losses in the tibia in a group of three monkeys restrained for 6 months. Relatively large losses of cortical bone are seen mainly in the anterior, proximal tibia. Thus, the losses appear not only to occur in typical weight-bearing bones, but also appear to be in the outermost cortical fibers which would be subject to stress levels during weight-bearing.

In a separate series of tests, the carbonate content of the tibia was found to decrease 7%, on the average, during short-term restraint. That reflects losses of the crystalline calcium carbonate-phosphate salts of the bone as well as a change in the total acid-buffering capacity of the body.

Mechanisms of Bone Loss

The balance between the rates of bone formation and bone resorption is a principal relationship which must be affected for a modification of bone mineral content to occur. Prior studies

(11) have shown that skeletal stressing achieved by intermittent or steady compression can produce local and regional bone hypertrophy by stimulating the endosteal and periosteal bone formation rate. Our experience with implantable bone strain gauges (12) indicates stress levels as high as 200 kg in the tibia of active monkeys; those levels are never approached during restraint. Consequently, the reduction of skeletal loading in our studies could have a significant effect on bone homeostasis.

Research efforts have also been focused upon elucidating the biochemical mechanisms which could give rise to bone loss through an increase in resorption rate. Other studies (13) have indicated that bone loss during hypodynamic immobilization is eliminated when the parathormone secreting system is removed, and consequently, that hormone is implicated in the bone loss observed during restraint.

In one experiment, our monkeys were evaluated during the course of 10-24 weeks of restraint. Figure 6 shows the rise in level of serum parathormone as determined by radioimmunoassay. The units shown are relative to a volume of a highly purified parathormone standard. The prerestraint values shown are similar to the normal human range, and the elevated levels are similar to those measured by an identical assay in patients with parathyroid adenoma who demonstrated a hypersecretory response (14).

In another experiment, three animals were observed for 24 weeks. Food intake (Purina) was held relatively constant and approached 180 g/day for each animal. Using the photon absorption technique, bone mineral losses of 4-6% were measured in the mid-shaft of the tibia. Bone loss was confirmed radiographically, with observation of thinning of the proximal tibial cortex and trabeculae in the calcaneus. Bone formation rate was determined using standard ^{47}Ca kinetics under metabolic balance conditions. The changes in critical calcium metabolism parameters are summarized in Figure 7. Bone formation rate in the control animals was 3.2 - 4.1 mg Ca/kg/day, compared to 7.2 - 13.2 mg Ca/kg/day after 6 months of restraint. Urinary phosphate of the control animals was 12 ± 6 mg/day; it was increased by a factor of 8 in restrained animals. Urinary hydroxyproline of the control animals was 5.2 ± 0.9 mg/day; it was doubled in restrained animals. Urinary calcium was 277 ± 103 mg/day in control animals; it was only modestly elevated, 17%, in restrained animals. The overall calcium turnover rate of the control animals was 377 mg Ca/day and was increased by 53% in restrained animals.

The data are consistent with the hypothesis that parathormone is implicated in hypogravic-hypodynamic bone loss. The increased urinary hydroxyproline and phosphate indicate an increased resorption rate of both the organic matrix and mineral phase of bone, and both are expected to occur with high levels of serum parathormone. Calcium turnover rate is the sum of calcium resorption from bone and intestinal dietary absorption. Dietary absorption, although it remained within normal limits in the restrained animals, was slightly depressed; therefore, the gross turnover rate was probably elevated because of a specific increase

in bone resorption. This provides further indirect evidence favoring the concept of an increased bone resorption rate. The bone formation rate was also increased in the restrained animals. Under clinical conditions of hyperparathyroidism, bone formation and resorption rates are coupled, and both increase during periods of severe bone loss.

The relatively low urinary calcium observed during long-term restraint is not surprising since parathormone itself reduces urinary calcium excretion (15). But, the possibility exists that calcium may be recycled in the body, rather than excreted, and deposited in a variety of tissues. Therefore, our on-going researches, in addition to evaluating specific endocrine involvement in bone loss, and parameters such as serum levels of ionic calcium and alkaline phosphatase, have also included evaluations of intracellular calcium distribution.

Requirements for several newer measurement techniques have been identified. First, it is important to apply a direct measure of bone resorption in our animal model system in order to establish unequivocally the change in that function during restraint. Second, it is desirable to measure skeletal bone mineral and calcium loss with a greater accuracy and convenience than is possible by metabolic balance techniques. Third, it is important to determine the effect of bone loss on the structural integrity of the skeleton.

NEWER EVALUATIONS OF THE SKELETAL SYSTEM

Bone Mineral Content

It has been apparent since the advent of single-photon absorptiometry that a dual-photon approach might be used to measure bone mineral content. The chief advantage of a dual-photon approach is in not having to surround the measured bone in a constant thickness of soft-tissue-equivalent material. In a dual-beam system, the attenuation of the radiation intensity in either air or soft tissue is slight but similar for the two distinct beam energies. On the other hand, absorption in bone is different for photons of different energy levels, and the differences are in proportion to the quantity of mineral present. Therefore, the ratio of the flux of the beam energies can be used to determine bone mineral content.

A prototype system utilizing a high-intensity (1 Ci) source of ^{153}Gd has been used to measure both vertebral and total body bone mineral in patients (16). Measurements are made on a modified Ohio-Nuclear whole-body rectilinear scanner. The ^{153}Gd (4 mm bead) is mounted below the scanning table, and a scintillation detector is mounted on the yoke above the subject. The beam size at the body level is less than 1 cm. The source and detector move simultaneously in a raster pattern.

The ^{153}Gd source emits at two energies (44 and 100 keV), and the attenuation is essentially linear when correction is made for the spillover from the higher to the lower energy channel.

Vertebral bone mineral is measured from L4 (lumbar) to T12 (thoracic) with a scan speed of 2.5 mm/sec and with 12.5-mm steps between scans. For measurement of total body mineral, the entire body area is scanned at a speed of 10 mm/sec with step intervals of 25 mm.

The radiation exposure measured by means of thermoluminescent lithium fluoride crystals is 2.1 mrad, with the majority delivered to the skin. The low dose level permits repeated scans without jeopardy to the patient.

The precision of vertebral scans in vivo averages 2.3%; measurement precision of the bone mineral content of vertebral phantoms is 1.7%. The variation of total body mineral content measured in vivo is 1.9%, which approaches the precision obtained in vitro.

We have recently applied the technique to experimental monkeys. Figure 8 shows the positioning of one animal on the scanning table. A scan speed of 2.5 mm/sec was utilized with 10-mm steps between scans. Animals in the 10-12-kg weight range contained 210-265 g of bone calcium. The measurement precision determined in two standards was 2%; that precision was approached in vivo. Consequently, this method could be useful for tracking the time history of skeletal calcium losses.

Bone Resorption Rate

The direct measurement of osteolysis and bone resorption in man has been determined by monitoring ^{48}Ca levels in the blood and urine (17). The procedure is based upon measuring in blood or urine a stable, naturally occurring, calcium tracer, ^{48}Ca , which is liberated from the skeleton through resorptive processes. To implement the studies with our animal model, monkeys are fed standard test diets providing a known and relatively stable daily intake of total calcium. Diets designed for these studies provide 375 mg Ca/day. Typically, dietary calcium is 96.97% ^{40}Ca ; that is replaced in the diet by a calcium source which has been depleted of ^{48}Ca , i.e., a source which is 99.91% ^{40}Ca . The natural abundance of ^{48}Ca in the skeleton is 0.18%; during the feeding of diets depleted of ^{48}Ca , the isotope is released from the skeleton, and its abundance in the blood falls as it is excreted in the urine and is only partially replaced by release from bone. The blood level of the naturally occurring isotope, ^{48}Ca , is measured by neutron activation analysis. Aliquot samples are irradiated with a flux of 10^{13} neutrons/cm²/sec, and the ^{48}Ca is measured as ^{49}Ca , which has a half-life of 8.7 min. Figure 9 demonstrates the nature of the data obtained with monkeys. There is an early exponential decline of ^{48}Ca level in the urine; after 2 weeks, an asymptotic abundance is reached which is the fraction of the total calcium turnover rate derived specifically from bone resorption. From Figure 9 it is inferred that 50% of turnover is derived from skeletal resorption, and therefore, 50% is derived from dietary calcium absorption. Measures of blood level ^{48}Ca provide substantially similar data, but with less precision because of the

low concentrations and relatively small blood samples. The current approaches address themselves to dietary enrichment studies in which monkeys are supplemented with 12 mg ^{45}Ca daily; serum levels increase exponentially to an asymptote; the results are interpreted essentially the same as in the prior approach, and there is a significant improvement in precision.

Bone Bending Rigidity

An experimental technique and the associated apparatus for measuring in vivo the mechanical impedance of the human ulna have been described in detail (18). An electromagnetic shaker is used to apply a steady-state harmonic excitation to the ulna near its midspan, and measurements of the complex driving-point impedance are made. With moderate restraint at the joints, the resistance to rotation is small, and the interosseous space is sufficiently large to avoid significant lateral contact with adjacent bones. At low frequencies, the bones behave as "simply-supported" beams immersed in a viscous fluid. The impedance probe is placed against the skin; with a preload of 600 g, the skin has a significant stiffness, although inconsequential mass. The velocity of the probe produced by a prescribed force yields data from which the bone stiffness can be separated from the skin stiffness with an accuracy of 10%. The absolute impedance of bone is determined for the responses below the first resonance, ~ 400 Hz. The spring constant k is the product of the impedance and frequency. The average bending stiffness EI is derived from the spring constant. Studies with excised bones tested to fracture in three-point loading show a high correlation, $r = 0.96$, between the bending stiffness and the maximum moment at fracture. Consequently, the parameter EI is a sensitive indicator of changes in the modulus E or in the cross-sectional moment of inertia I which would alter the mechanical integrity of bone.

Figure 10 demonstrates the measurement of impedance in the tibia of a monkey. The probe is placed at the midspan of the tibia. Typical values for the average bending stiffness of the tibia are on the order of 11×10^9 dyne-cm². The general approach described above can be applied to assess the effect of local areas of bone demineralization on structural integrity.

The approaches described above and the data base obtained through laboratory experiments indicate that the monkey is a useful test model for the evaluation of certain types of human calcium problems. For that matter, experiments with monkeys may also be a useful adjunct for studies of general metabolic responses, the control of red blood cell mass and plasma volume, and perhaps cardiovascular dynamics in relationship to hypodynamic environments. However, theories and mechanisms concerning the biology of weightlessness can be tested only in a limited fashion in ground-based studies. Eventually, it is necessary to determine that reactions predicted on the basis of simulation experiments do in fact occur in true weightlessness. The design and evaluation of

equipment and holding facilities for future experiments with monkeys thus are critical developmental requirements.

PRIMATE FLIGHT EXPERIMENT SIMULATION AND IMPLEMENTATION

Among the facilities to be developed and used for a variety of space life sciences experiments, three are applicable to the investigations discussed here: a primate holding facility, a primate transporter, and a surgical workbench.

Holding Facility

Primate caging and experimental facilities are currently under development for a spacelab life sciences laboratory simulation. Termed Spacelab Simulation Development III (SMD III), it is scheduled for operation in May 1977. Ames Research Center has the integration and development responsibility for a number of biological experiments, the actual simulation to be conducted at and with the support of Johnson Space Center. The test is to be of 7 days duration.

Two primate cage designs have been completed by Lockheed Missiles and Space Co. (19) and McDonald Douglas Corp. (20). A composite of the two designs is illustrated in Figure 11. Note that the unit is integral with a standard Spacelab rack 105 cm wide, 275 cm high, 72 cm deep at maximum depth.

The primate cage was configured to afford ample living space for an unrestrained 11-14-kg primate and to provide an optimal life support situation. The inside dimensions of the cage are approximately 64 x 64 x 95 cm. Food and water are supplied by a hopper and a lixit valve/reservoir system, respectively. Water dispensed is automatically measured, while food is replaced manually.

Collection of feces is handled by a 6.4-mm mesh screen placed about 15 cm beneath the floor of 6.4-mm rods spaced 38 mm apart. Urine is collected and dried on an underlying phosphoric-acid-impregnated pad. Both incoming and outgoing air is filtered through a 0.5-micron (87% efficient) H.E.P.A. filter. Outgoing air is also filtered through a charcoal bed. The sizing of the waste collection bed permits storage over the mission duration, although ready access allows cleaning and changing if desired. Feces can be readily collected throughout an experiment course.

Fluorescent lighting may be programmed to a required daily regime, while visibility is afforded by the vertical Plexiglass window. Ambient lighting may be controlled by a Velcro-fixed cloth curtain across the window.

Temperature control depends upon spacelab ECS (Environmental Control System) inlet temperatures. The SMD III will provide 16°C air through a ceiling vent located about 2.5 cm from the inlet to the primate holding facility. This air, termed process air, is collected by a blower which provides bleed air to a separate, fan-driven air circulation loop entering the cage from the top and moving linearly down through the cage at the rate of

60 ft³/min. This cage circulation air with process air is vented from the front bottom of the facility. Temperature is sensed in the process air loop, driving the differential opening or closing of a solenoid actuated valve to control habitat temperature.

Preliminary tests showed that a 12-kg macaque contributes about a 4°C differential, necessitating the inclusion of a resistance heater in the system with air inlet temperatures as low as 16°C.

Transporter

Consideration of constraining mission operations indicated problems in inserting the primate in the holding facility before launch. The approach has been, therefore, to board the monkey in the orbiter a few hours prelaunch, carry it there through the launch phase, and to insert it in the spacelab soon after achievement of orbit. General Electric Co. was contracted to fabricate a primate transporter with this purpose in mind for SMD III. The design was conceived in a prior study (21). It provides a 2-day food and water supply and a self-contained air circulation capability. Since it is to operate in the benign orbiter environment, sophistication of design was minimal. It is illustrated in Figure 12.

The holding facilities and transporters have been designed with appropriate interfaces to facilitate primate transport. When joined to the front of the cage, the doors of transporter and cage are commonly opened, and the ceiling of the transporter is moved down to effect the transfer. To move an unanesthetized animal from the cage, a manually operated squeeze wall mechanism forces the primate into the transporter. An anesthetized animal may be removed by opening the hinged cage front. Access for syringe intramuscular injections is provided by the barred partition in the cage transfer port in conjunction with manipulation of the squeeze wall.

Surgical Workbench

The use of a third facility in SMD III (as well as for flight) is required by this experimentation. A surgical workbench will be used for a number of life sciences functions, e.g., microbiological tasks, sample transfers and measurements, dissections, perfusions, microscope observations, and photography, etc. (22). The design concept is illustrated in Figure 13. Here, as with the primate cage, the double rack is used. It will provide a restraint capability and work space for the anesthetized monkey while blood samples are taken. It also provides a linear airflow and lighting. Contained within a double rack, the working chamber may be extended into the spacelab aisle allowing access through glove ports from both sides. Access for some applications may be directly through the Plexiglass front when it is folded into the top. A downward flowing air current of sufficient velocity across the front insures atmospheric isolation with the front in this

position. A water reservoir and flexible plumbing constitute a wash-down system with waste water collected through the perforated Plexiglass floor by a vacuum/reservoir system; electrical outlets within the chamber service appliances when needed.

Investigations with unrestrained primates, then, will be implemented in spacelab simulations by the use of these three facilities. The following sequence of operations is planned.

Shortly before test start, the monkey will be transferred from the laboratory to the simulated orbiter by transporter. The transporter will, at some time after scheduled orbit, be moved to the spacelab and joined to the holding facility. When transfer has been effected, water consumption and food intake will be monitored, and feces collections will be made on a predetermined schedule. The animal will be anesthetized daily and removed to the surgical workbench where the required treatments and sample taking will be performed. On the last simulation day, by use of the squeeze-wall mechanisms, the animal will be transferred to the transporter for placement in the orbiter while reentry and recovery operations ensue. Postrecovery observations will begin after removal from the orbiter to the ground laboratory.

SUMMARY

Experimental approaches in the development of the monkey as a useful test animal for the evaluation of calcium metabolism have been reviewed. The measurement of total body calcium by photon absorption techniques, the measurement of skeletal resorption rate, and the measurement of bone stiffness have been shown to be feasible and can provide useful information regarding skeletal status. The configuration of developmental primate life support equipment and its application in spacelab simulation programs have been discussed.

ACKNOWLEDGMENT

The contributions of John K. Jackson and Mahmood Yakut of McDonald Douglas Corp., Bruce Maine of Lockheed Missiles and Space Co., Ted Aepli and Roy Smith of General Electric Co., and William E. Berry and Paul X. Callahan of Ames Research Center are gratefully acknowledged in the design of the implementing hardware. The contributions of Chris Cann are acknowledged for some of the physiologic studies.

REFERENCES

1. Whedon, G. D., L. Lutwak, P. Rambaut, M. Whittle, C. Leach, J. Reid, and M. Smith: Effect of weightlessness on mineral metabolism; metabolic studies on Skylab orbital space flights. *Calcif. Tiss. Res.*, 21:423, 1976.
2. Kazarian, L. E., and H. E. Von Gierke: Bone loss as a result of immobilization and chelation. Preliminary results in *Macaca mulatta*. *Clin. Orthopaed. and Related Res.*, 65:67, 1969.

3. Kazarian, L. E., and H. E. Von Gierke: Age and exercise as factors influencing osteoporosis, bone strength and acceleration tolerance. Proc. AGARD Conf., 82:8, 1971.
4. Young, D. R., G. A. Thompson, W. H. Howard, R. R. Adachi, and L. Lutwak: Short-term blood calcium regulation in the monkey. Indian J. Nutr. Dietet., 12:243, 1975.
5. Bell, N. H., R. J. Barrett, and R. Patterson: Effects of porcine thyrocalcitonin on serum calcium, phosphorus and magnesium in the monkey and man. Proc. Soc. Exp. Biol. Med., 123:114, 1966.
6. Raman, A.: The effects of thyrocalcitonin on ionic and total plasma calcium in monkeys. Horm. Metab. Res., 3:48, 1971.
7. Harris, R. S., J. R. Moor, and R. L. Warner: Calcium metabolism of the normal rhesus monkey. J. Clin. Invest., 40:1766, 1961.
8. Neer, R., M. Berman, L. Fisher, and L. E. Rosenberg: Multi-compartmental analysis of calcium kinetics in normal adult males. J. Clin. Invest., 46:1364, 1967.
9. Howard, W. H., J. W. Parcher, and D. R. Young: Primate restraint system for studies of metabolic responses during recumbency. Lab. Anim. Sci., 21:112, 1971.
10. Sorenson, J. A., and J. R. Cameron: A reliable in vivo measurement of bone mineral content. J. Bone Joint Surg., 49-A:481, 1967.
11. Chamay, A., and P. Tschantz: Mechanical influences in bone remodelling. Experimental research on Wolff's Law. J. Biomechan., 5:173, 1972.
12. Young, D. R., W. H. Howard, and D. Orne: In vivo bone strain telemetry in monkeys (*M. nemestrina*). J. Bioeng., in press.
13. Burkhart, J. M., and J. Jowsey: Parathyroid and thyroid hormones in the development of immobilization osteoporosis. Endocrinology, 81:1053, 1967.
14. Reiss, E.: Analyses and measurements of blood samples. NASA CR-1395, 1969.
15. Agus, F. A., L. B. Gardner, L. H. Beck, and M. Goldberg: Effects of parathyroid hormone on renal tubular reabsorption of calcium, sodium and phosphate. Amer. J. Physiol., 224:1143, 1973.
16. Madsen, M., W. Peppler, and R. B. Mazess: Vertebral and total body bone mineral content by dual photon absorptiometry. Calcif. Tiss. Res., 21:361, 1976.
17. Hansen, J. W., G. S. Gordon, and S. G. Prussin: Direct measurement of osteolysis in man. J. Clin. Invest., 52:304, 1973.
18. Thompson, G. A., D. Orne, and D. R. Young: In vivo determination of mechanical properties of the human ulna by means of mechanical impedance: experimental results and improved mathematical model. Med. Biol. Eng., 14:253, 1976.
19. Conceptual design for a biological specimen holding facility. Final Report, LMSC DOS6047, Vol. I, Lockheed Missiles and Space Co., Inc., June 1976, Prepared under contract no. NAS8-31491.

20. A conceptual design study of a biological specimen holding facility. Final Report, MDC 66203, Vol. II, McDonnell Douglas Corp., May 1976, Prepared under contract no. NAS8-31490.
21. Biomedical experiments scientific satellite. Preliminary design study, Vol. I, General Electric Co., 1976, Prepared under contract no. NAS2-8896.
22. Callahan, P.: Personal communication.

TABLE 1

Effect of 10 Weeks of Restraint on the Average Daily Urinary Nitrogen, Potassium, and Phosphorus in Monkeys^a

Test monkeys	Urinary nitrogen, mg/day	Urinary potassium, mg/day	Urinary phosphorus, mg/day
Restrained animals (4) ^b	3389 ± 1337 ^c	661 ± 312 ^d	82 ± 53 ^e
Pair-fed controls (4)	2747 ± 558	540 ± 92	17 ± 30

^aValues are means ± S.D.

^bValues in parentheses are numbers of animals.

^cSignificantly different from control animals, $p < 0.01$.

^dSignificantly different from controls, $p < 0.02$.

^eSignificantly different from controls, $p < 0.002$.

TABLE 2

Tibia Mineral Content During One Month of Restraint^a

Prerestraint	Postrestraint	% Diff
0.61	0.60	-1.64
0.71	0.71	0
0.76	0.74	-2.63
0.80	0.70	-12.50
1.02	0.97	-4.90
0.93	0.95	+2.15
0.84	0.81	-3.56
0.79	0.74	-6.33
1.07	1.03	-3.74
0.99	0.97	-2.02

^aValues are g/cm; $\bar{x} = -3.50\%$;
 $t = 2.88$; $p < 0.05$.

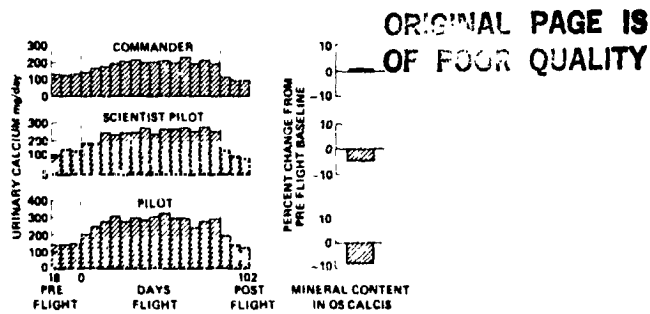


Fig. 1.- Urine calcium and bone mineral loss from os calcis during the 84-day Skylab 4.

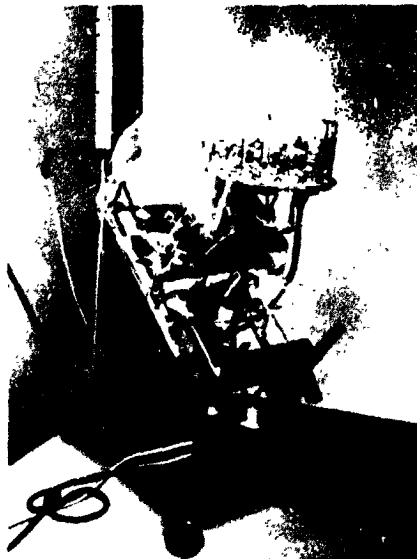


Fig. 2.- Primate restraint unit showing arrangement of equipment and animal as used in these studies. Provisions are for watering and feeding and for the collection and refrigeration of urine samples.

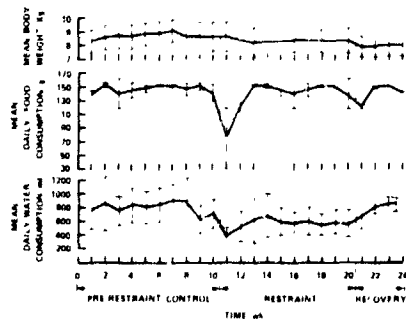


Fig. 3.- Body weight, food consumption, and water intake of seven monkeys during control, restraint, and recovery periods. Values are means \pm S.D.

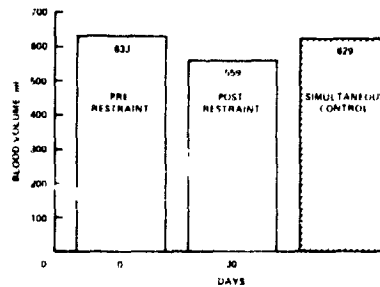


Fig. 4.- Blood volume changes in three restrained monkeys.



Fig. 5.- Losses of cortical bone in the tibia during restraint. Animal #35 was restrained for 6 months. Significant losses of cortical bone occurred in the proximal-anterior tibia. Animal #37 was a control animal.

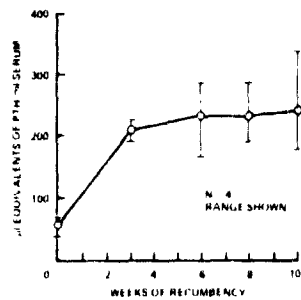


Fig. 6.- Increase in serum level of parathormone during restraint in monkeys.

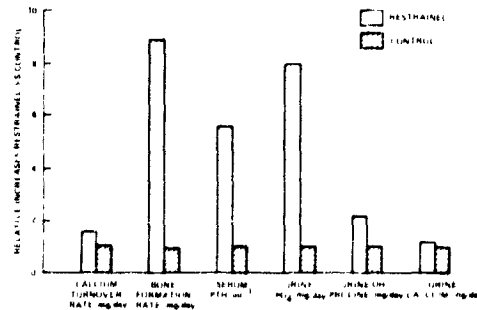
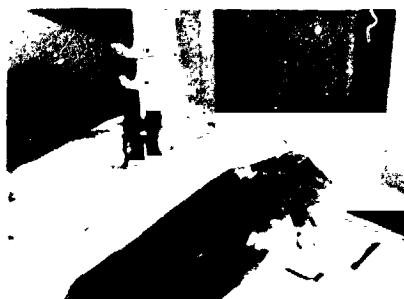


Fig. 7.- Effect of long-term restraint on several calcium metabolism parameters. The relative increase observed in restrained animals is shown on the vertical scale.



ORIGINAL PAGE IS
OF POOR QUALITY

Fig. 8.- Measurement of total skeletal mineral content in the monkey utilizing dual photon absorptiometry are made under anesthesia to avoid motion.

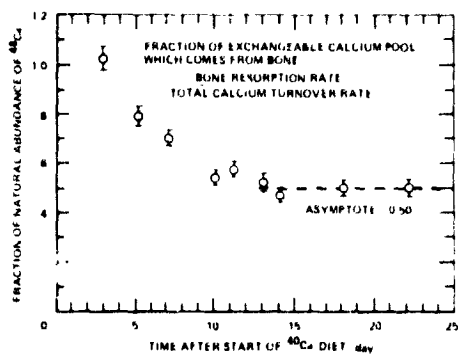
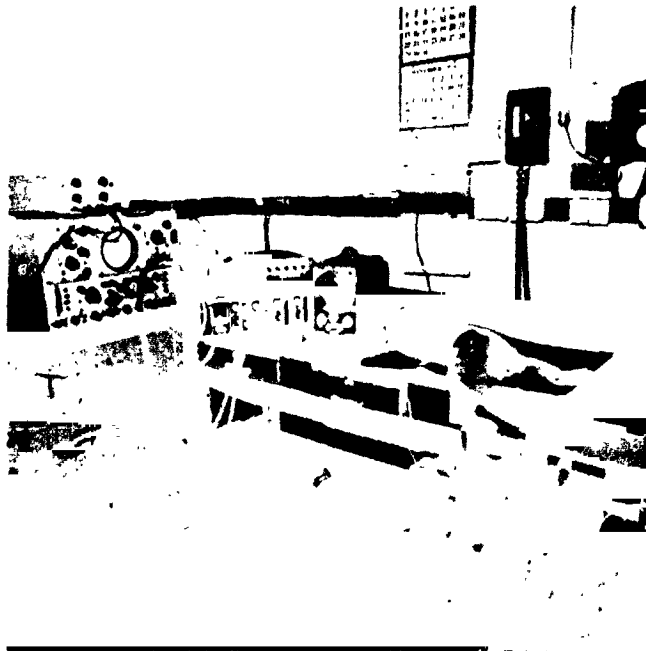


Fig. 9.- Measurement of the fraction of exchangeable calcium arising from bone resorption in the monkey. ^{48}Ca in urine is measured by neutron activation analysis.



MONKEY 37 LEFT TIBIA

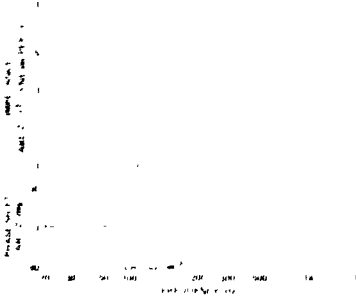


Fig. 10.- In vivo measurement of the impedance of the tibia in a monkey.

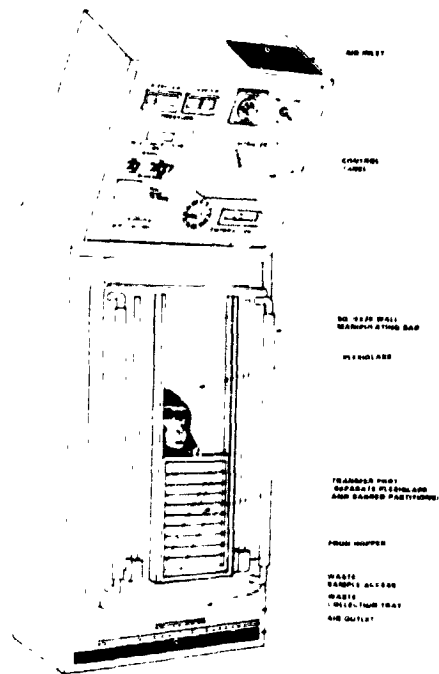


Fig. 11.- Primate holding facility design concept. Control panel is shown in an expanded front view for clarification purposes.

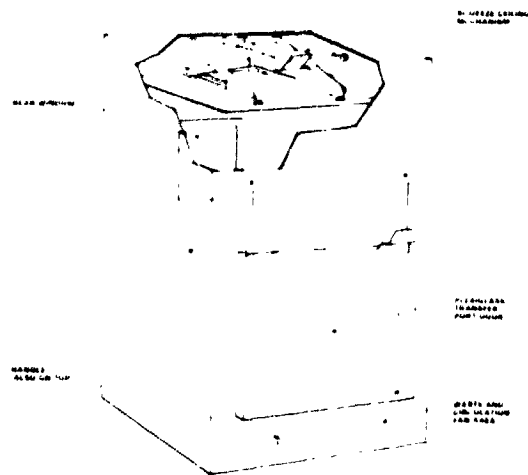


Fig. 12.- Primate transporter design concept.

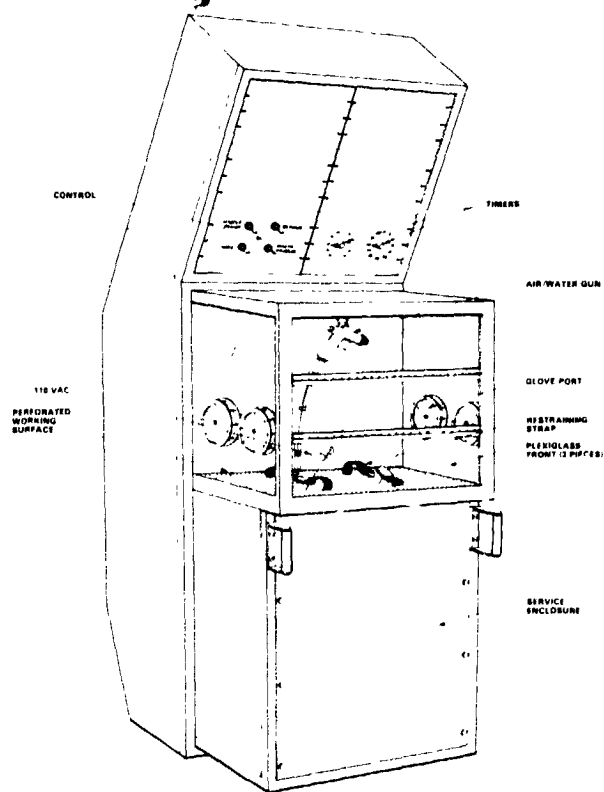


Fig. 13.- Surgical workbench design concept.

ORIGINAL PAGE IS
OF POOR QUALITY